Nov 8th, 12:00 AM

Repeated Point Loading on Composite Slabs

Laurence A. McCuaig

R. M. Schuster

Ninth International Specialty Conference on Cold-Formed Steel Structures
St. Louis, Missouri, U.S.A., November 8-9, 1988

REPEATED POINT LOADING ON COMPOSITE SLABS

by

Laurence A. McCuaig* and Reinhold M. Schuster**

SUMMARY

Composite slabs have been and still are primarily used in office and apartment buildings where the design load is based on equivalent uniformly distributed static loading. The use of composite slabs in the construction of warehouses and indoor parking garages has been limited due to the lack of behavioural and strength information of composite slabs subjected to repeated point loading. This paper presents test results of an experimental study recently carried out at the University of Waterloo on composite slabs subjected to repeated point loading. Based on these tests, both simple and double span specimens were able to sustain repeated point loads of 55% of static ultimate for at least 1.25 million cycles. The mode of failure in all cases was by metal fatigue in the steel deck.

*Lorlea Steels, Formerly Graduate Student, University of Waterloo, Waterloo, Ontario, Canada.
**Associate Professor, Department of Civil Engineering and School of Architecture, University of Waterloo.

INTRODUCTION

Steel-deck reinforced concrete slabs or "composite slabs" consist of cast-in-place concrete on cold-formed corrugated and/or ribbed steel decking (see Figure 1). For most applications, such as office and apartment buildings, composite slabs are subjected primarily to static loading. However, in structures such as warehouses and parking garages, where repeated concentrated loading can occur, fatigue is a likely source of failure. Fatigue failure results from concentrated loads which are varied or repeated, each load being smaller than the single static load which would cause failure. Many structures are subjected to repeated loads and although the average stresses may be low, local concentrations of stress, which have negligible effect on static strength, can often lead to failure by fatigue.

The purpose of this paper is to present results of a composite slab system subjected to concentrated repeated point loading. The study was carried out by McCuaig [17] at the University of Waterloo, under the auspices of the Canadian Sheet Steel Building Institute (CSSBI) and was a continuation of the study by R. Suleiman [15].

Traditionally, composite slab research has concentrated on the effect of static loading and several papers have been published on this topic [1,2,3,4,8]. Test data clearly show that under static loads, ultimate failure is related to a combination of diagonal tension shear failure and steel-concrete interface bond failure. The result is a failure mode commonly referred to as "shear-bond". The shear-bond resistance of a particular composite slab system depends upon size, depth, orientation of embossments, surface coating, etc. and thus, varies for each manufacturer's product. Several design expressions have been developed to describe the shear-bond failure mode [2,3,7,8]. To date, the technical literature does not contain conclusive information on the effect of repeated loads on composite slabs; however, some noteworthy studies related to this topic have been published [9,10,11,12,14,15,16]. Although the method of loading the specimens in each of the above-noted studies varied from central line loading to four symmetrically oriented point loads, the mode of failure due to repeated loading was usually shear-bond. In this study, the primary mode of failure due to repeated loading was metal fatigue in the steel deck.

TEST PROGRAM

Ten single and three double span composite slab specimens were tested under both static and repeated concentrated point load conditions. The static load tests were conducted to ultimate failure and the results were used to form the basis for the selection of repeated load levels in the fatigue tests. A desired fatigue life of 1.25 million cycles was established by an Ad-Hoc committee under the auspices of the research sponsor (Canadian Sheet Steel Building Institute) as a reasonable limit for warehouse applications.

Description of Test Specimens

Of the ten single span specimens tested, nine consisted of two steel deck panel widths and one was constructed using a single panel only. The double width specimens were 2250 *mm* long × 1830 *mm* wide with an average slab depth of 150 *mm*. The single width specimen was identical except that the width was only 915 *mm*. The specimens were designed such that a span of 2150 *mm* existed between support centres. Three double span specimens were constructed with overall slab dimensions of 4400 *mm* long × 1830 *mm* wide with an average slab depth of 150 *mm*. The individual span length between supports was 2150 *mm*. For both single and double

span specimens, steel bearing plates were welded to the bottom of the steel decks at the end of each specimen (and at the centre of the double span specimen). The bearing plates were designed with a width of 75 *mm* to satisfy the minimum field practice requirement of being equal to or greater than the deck depth. This was done to provide a smooth bearing surface for the transfer of loads to the supports.

Materials used to construct the test slabs consisted of cold-formed steel decking, welded wire fabric, and concrete. All materials were used in "as received" condition to ensure that the behavioural characteristics of the composite slabs would not be altered from that expected under normal service conditions.

Composite steel decks were nominally 75 *mm* in depth and 0.91 *mm* in thickness (see Figure 2). Since two different shipments of deck were received from the manufacturer during the study, some variation in thickness and embossment depth was experienced. All steel decks were supplied with a zinc-coated surface finish and had mechanical properties in conformance with ASTM A446M-80 Grade A material.

Normal density concrete with a minimum compressive strength of 20.7 MPa, was supplied by a local ready-mix plant. The specimens were cast with supports at regular intervals along their entire length. This does not normally occur in field installations where shoring is generally not required during casting and, when it is required, is usually restricted to supporting the deck at midspan only. The deflection caused by the wet concrete (ponding) on unshored decks increases the depth of the composite section in actual construction practice. This additional depth, and consequently additional stiffness, is generally disregarded in design and the nominal depth is utilized in strength calculations. Under static loading conditions, slightly conservative results are usually obtained when continuous shoring is provided. Welded wire fabric consisting of No. 6 wires (152 *mm* × 152 *mm*) was used as supplementary reinforcement in all slab specimens.

Test Equipment and Instrumentation

The load train consisted of a test frame, specimen and drive system. All tests were conducted in a large, self-contained load frame. The drive system utilized an MTS Electrohydraulic Servo Unit operating under closed-loop control, allowing the loads transferred to the specimen to be controlled and maintained on a continuing basis.

The test set-up for the single and double span specimens is shown in Figure 3 and Figure 4, respectively. Loading was accomplished by applying a concentrated load at the geometrical centre of the specimen. A 200 *mm* square steel plate was used to simulate the size of a fork-lift truck wheel and a 25 *mm* thick neoprene pad was placed between the plate and the contact surface of the concrete to provide a uniform bearing surface between the concrete and the applied load.

Instrumentation consisted of mechanical dial gauges, displacement transducers (LVDT's) and electrical strain gauges. These devices were used in monitoring specimen behaviour through various recording devices. As shown in Figure 3, the dial gauges and LVDT's were positioned along the midspan centreline, at the centre of the support beams, and at the centre of the unloaded span in double span specimens. Additionally, for static testing only, one LVDT and two dial gauges were placed at each end of the specimens to record horizontal end-slip.

Strains were measured at critical locations on the bottom of the steel decks by attaching single axle strain gauges to the steel surface. In general, gauges were placed over only one-half of the specimen width on flat areas of both the top and bottom flanges of the deck bottom

surface. Strain gauges were placed along the transverse midspan centrelines of both loaded and unloaded spans, and for double span specimens, strain gauges were also placed on the steel deck along the interior support beam.

Test Procedure

Static tests were conducted to determine the ultimate load and mode of failure, as well as to observe the behavioural characteristics of the specimen when subjected to a concentrated point load. Based on the results of these tests, the maximum loads for repeated point load testing were established. This was done by applying a weighted load factor to the ultimate failure load as follows:

$$P_{mr} = \frac{P_{ue}}{WL}$$

The weighted load factor, WL, was established using the dead and live load factors specified in CAN3-A23.3 [20], hence,

$$WL = \frac{1.4P_D + 1.7P_{ue}}{P_D + P_{ue}}$$

In all tests a load ratio of 0.1 was chosen for testing, that is, a minimum repeated load equal to ten percent of the maximum repeated load was chosen to define the load cycle. This was done to avoid excessive vibrations which result when each cycle ranges between zero and the maximum repeated load. Repeated load testing was conducted with cyclic frequency of 3 Hertz throughout the majority of all tests.

TEST RESULTS

It is not the intention of this paper to discuss the results of each individual test, but rather to present some typical results and to briefly summarize the findings of this research. The reader is referred to Reference [17] for more detailed information.

Static Tests

The results of the five static load-deflection tests are summarized in Table 1. Shear-bond was the failure mode in all cases and was characterized by horizontal end-slip between the steel deck and concrete, followed by a loss in load-carrying capability and an excessive amount of vertical deflection at midspan. End-slip only occurred at ultimate load, i.e., no early end-slip was observed for this particular deck product. In all cases, shear-bond failure was preceded by yielding of the steel deck, but in no case did yielding extend into the top flanges of the steel deck.

End-slip was abrupt and increased to the maximum measured value almost immediately, after which no further slippage took place. End-slip was measured at both ends of each single and double span specimen and at only one end of the single-width specimen R-1-SS-SW. The greatest end-slip was experienced with specimen R-2-SS which failed at a lower load (88% of that achieved for specimen R-1-SS) than other specimens and experienced a greater amount of observable bending in the transverse direction perpendicular to the corrugations of the steel deck. Unlike other specimens, specimen R-2-SS failed prior to yielding of the bottom fibres of the steel deck over the entire slab width, although some yielding was experienced near the centre of the slab in the immediate vicinity of the concentrated load.

The single span specimens R-1-SS and R-2-SS, failed at an average ultimate load of 105 *kN*, whereas both double span specimens, R-1-DS and R-1-DS-A, failed at loads approximately 11.4% greater (117 *kN* for both). This indicates that continuity over the interior support gives some benefit when composite slabs are subjected to point loads. These results compare favourably with those obtained by Suleiman [15], where it is recorded that double span specimens achieved ultimate loads of approximately 8.8% larger than single span specimens.

The crack pattern observed at completion of the two single span specimens (R-1-SS and R-2-SS) was similar, which for specimen R-1-SS is illustrated in Figure 5. No flexural cracking was observed along the sides of the specimens in either case, although a large amount of bending had occurred before the tests were stopped (as is indicated by the yielding of the bottom flanges of the steel deck). The cracks observed on the top surface of all slabs illustrated the nature of the crack growth pattern prior to ultimate failure. Cracking originated at the central point load and propagated towards the supports as failure proceeded. In so doing, a "wedge" was formed which ultimately pushed out as the diagonal tension crack formed near the point load, resulting in the loss of the mechanical interlocking capacity between the concrete and embossments of the deck. The end cracks originated at the corner of one of the top flanges away from the centreline of the specimen, and formed an angle of approximately 45 degrees to the horizontal. This crack pattern indicates that when composite slabs are subjected to concentrated point loads, shear-bond failure occurs over an "effective-width" of the specimen. This is similar to the behaviour observed by Porter [13].

The shear-bond failure was substantiated in observations of end-slip at failure which was confined to the central portions of the slabs. The crack patterns observed for the double span specimens were similar in nature except that the wedge formed only towards the free end of the specimen and cracking occurred over the interior support across the entire slab width.

The crack pattern observed for the single-width specimen R-1-SS-SW was much different in that flexural cracking was observed on both sides of the specimen prior to the development of the major diagonal tension crack, which is normally associated with a shear-bond failure. This cracking pattern is similar to that observed for typical composite slab specimens subjected to line loading [2,5,8], indicating that the load was distributed completely across the width of the specimen. The effective width concept is further illustrated by examining the load per unit width column in Table 1. An ultimate failure load of 71.8 *kN/m* was experienced for the single width specimen, which is 15% greater than that obtained for specimen R-1-SS.

With the exception of specimen R-1-DS-A, all specimens failed at approximately the same midspan deflection. In the case of specimen R-1-DS-A, it is believed that compressive stresses developed in testing the other span were also present at the beginning of this test. An initial upward deflection, due to pre-compression resulting from testing on the opposite span, accounts for much of the observed difference in deflections.

Repeated Load Tests

The results of the repeated load tests of both single and double span specimens are summarized in Tables 2 and 3, respectively. Selection of load levels that were used on successive tests was based on a testing procedure which was a combination of the "staircase" method for fatigue testing and the "step-testing" technique for conducting individual tests. By using this approach, load levels for successive tests were based upon the success or failure of the previously tested specimen. This is a common method for full-scale fatigue testing where the main objective is to

establish the fatigue strength of a specimen based on a desirable fatigue life.

Failure Mode

Embossment fatigue in the steel deck was the cause of failure under repeated point loading with all specimens. Failure was characterized by the formation of a crack across the bottom flange of the steel deck perpendicular to the longitudinal direction of the deck corrugations. In all cases, fatigue cracks originated and propagated from an embossment located on the bottom flange of the steel deck near the point of loading. Figure 7 shows a close-up view of a typical fatigue crack. The photograph was taken on the bottom surface of specimen R-3-SR and was typical for all cases, in that the fatigue cracks tended to follow a row of embossments adjacent to the original crack location. This observation was substantiated in studies [9,16] of composite slabs subjected to repeated line loading, where the same observation was made for a different product type which also failed due to embossment fatigue. It should be noted that Temple's specimens also had embossments located on the bottom flange, resulting in the development of a fatigue crack due to the localized increase in steel stresses.

Fatigue failure was defined when the number of cycles were reached that initiated and propagated a crack across the entire width of one steel deck bottom flange. Only at this stage can a fatigue crack be readily detected. This degree of cracking generally results in a loss of stiffness in the composite slab and an increasing rate of deterioration. In all cases, the cracks developed near the midspan of the specimen.

Analysis of Stress Concentrations

The stress raisers created by the embossments were the location for the initiation and propagation of all fatigue cracking. Microscopic examination of a fatigue failed deck specimen revealed that the cracking was initiated at the "sharp" bottom corner of the embossment and propagated along the embossment into the flat portion of the deck. Further examination revealed that after the initiation of the fatigue crack, the crack increased in length by the "tearing" action created by cycling.

The elastic stress concentration factor, K_t, was determined by comparing the elastic strains and stresses measured with companion strain gauges before fatigue cycling began. The companion strain gauge consisted of a gauge for measuring the nominal deck strains, Δe, which was placed on the flat portion of the deck, and nearby, a small strain gauge to monitor the local strains, $\Delta\varepsilon$, was placed at the root of an embossment. By using these values, the elastic stress concentration factor was determined from:

$$K_t = \frac{\Delta\sigma}{\Delta S_n}$$

where $\Delta\sigma$ is the elastic stress directly adjacent the embossment and ΔS_n is the nominal stress in the deck. Care was taken to ensure that only elastic strains were used to calculate K_t. In cases where the local strain was greater than the proportional limit of the steel, the values were not used in the analysis. The results are shown in Figure 8, in which the local stress is plotted against the nominal stress for selected specimens. Specimens R-6-SR to R-9-SR were instrumented with the small strain gauges which were placed as close as possible to the embossments. The slope of the straight line fit to the test results represents the elastic stress concentration factor, K_t. The plot shows that the data from several different groups of gauges fit the straight line

plot reasonably well. The elastic stress concentration factor, K_t, was determined to be 2.1 for the embossment type tested.

Cracking

No flexural cracking in the concrete was observed in any of the specimens. In some cases, diagonal end cracking was observed at the support beams. However, no end-slip was observed at any time in any of the specimens. The cracks were similar to those developed under static loading. In double span specimens, if the crack over the interior support did not occur during the initial static cycle, concrete cracking occurred over the interior support beam after the first few cycles.

Deflections

As in previous studies by Mouw [12], Temple [9,16] and Suleiman [15], most of the increase in permanent deflection occurred prior to the first 100,000 cycles. Following 100,000 cycles, the rate of deflection increase with the number of cycles usually became stable until fatigue failure was observed. This was true for all specimens with the exception of specimen R-6-SR which appeared to experience damage on the first static cycle and continued to deteriorate at an increasing rate until failure occurred at 200,000 cycles. The remainder of the deflection-log cycle relationships show a relatively small increase in deflection with time, resulting in essentially a flat curve until fatigue failure. At failure, the deflection-log cycle curve increased abruptly until the test was stopped.

Permanent deflections (permanent or "irrecoverable" deflection refers to the measured deflection when no additional load is being applied at any time during cycling) ranging from 1.84 to 3.02 *mm* were measured for single span specimens, depending on the amount of cycling and damage the specimen had withstood. Double span specimens had measurable permanent deflections which extended over a similar range (1.86 to 3.44 *mm*) at the time the test was stopped. This can be misleading since double span specimens were generally cycled at higher loads and for longer periods of time than single spans. Comparison of companion specimens R-8-SR and R-2-DR gives a more accurate view of the advantages provided by continuity over an interior support. Both specimens were subjected to the same load for the same number of cycles and had similar concrete strength properties prior to testing. At completion of the test, the single span specimen R-8-SR had a measured deflection at zero load of 2.44 *mm* as compared to 1.87 *mm* for the double span specimen.

Coaxing

The favourable effects of coaxing were evident with specimens which had been subjected to a previous load history below the fatigue limit. Figure 9 illustrates this effect on specimens R-4-SR and R-5-SR, which were subjected to the same repeated loading cycle. Specimen R-4-SR however, had been previously subjected to 1.25 million cycles at a load below the fatigue load limit. As can be seen, specimen R-4-SR was subjected to the total fatigue life at the increased load with negligible increase in deflection. On the other hand, specimen R-5-SR failed after 725,000 cycles. Coaxing is also evident in comparison of specimens R-2-DR and R-2-DR-A. This behaviour is not surprising since coaxing is a property common to both concrete and steel, as well as with composite slabs. Studies on metals have shown that coaxing can be attributed to strain aging of the metal; the same is thought to be true for plain concrete [18].

The coaxing phenomenon was also quite evident in the earlier tests conducted by Suleiman [15]. In repeated load tests of companion specimens, a specimen with no previous load history was subjected to a maximum repeated load of 74% of ultimate static failure load and failed at 18.2 *Kc*. In comparison, the companion specimen which had previously been cycled at maximum loads of 62 and 68% of ultimate static failure load, each for 1250 *Kc*, was able to sustain 1250 *Kc* at a maximum load ratio of 74%. On completion of the third successive runout there were still no apparent signs of damage.

Double vs. Single Span Specimens

The advantage of providing continuity over the interior support is evident in Figure 10 where the deflection-cycle relationship for specimens R-5-SR and R-2-DR are compared. Both specimens were subjected to the same repeated load, however the double span specimen, R-2-DR, had an initial deflection of 19% less than that experienced by the single span specimen R-5-SR. As a result, the stresses experienced by the steel deck were lower, hence a longer fatigue life can be expected. This is further evidenced by the failure of specimen R-5-SR after 725,000 cycles while specimen R-2-DR continued to be subjected to 1.25 million cycles with no apparent damage.

Ultimate Strength Following Fatigue Failure

Following the fatigue cycling process, each slab was subjected to a final static load-deflection test to failure. Prior to each test, the slab specimens had been damaged to various degrees by cycling, the results of which are summarized in Table 4. When tests were conducted immediately following the development of the first fatigue crack, the ultimate mode of failure was a combination of flexure and tearing of the steel deck. Failure was characterized by flexural cracking along the sides of the specimens accompanied by excessive midspan deflection. In none of the cases did end-slip occur, even though the maximum loads were comparable to those experienced by companion static test specimens (specimens R-1-SS, R-2-SS, R-1-DS and R-1-DS-A). These results have been observed by other researchers [9,12,15,16] and in some cases it has been concluded that cycling actually increases the ultimate static failure load. This is especially true for specimens which traditionally experience early end-slip, such as those tested by Mouw [12].

SUMMARY AND CONCLUSIONS

The test results of single and double span specimens are summarized in Figures 11 and 12, respectively. In each case, the results are expressed in terms of a load ratio versus the number of cycles to failure. The load ratio in this case, is the ratio of the maximum repeated load divided by the ultimate first-cycle static load of the composite slab. Included are also the test results obtained by Suleiman [15]. It appears that the results could be fitted to a standard S-N curve, although the number of tests are too small to state this conclusively.

For single span specimens, it can be stated that the fatigue limit is approximately 55% of the ultimate static failure load. This is equivalent to a concentrated load of 60.0 *kN*. Failure is likely to occur before 1.25 million cycles at significantly greater loads. The fatigue limit for double span specimens is increased to approximately 60% of the ultimate static failure load. This translates to a maximum concentrated load of 70 *kN*, representing a 16.7% increase over that achieved by cycling single span specimens. This indicates that continuity over the interior support provides a beneficial effect when composite slabs are subjected to repeated point

loading. Although the double span specimens were cracked over the interior support beam, the continuity provided by the steel deck limited the amount of cyclic creep which occured during the test.

Based on Suleiman's tests [15], fatigue limits of 65 and 70% respectively, can conservatively be estimated for single and double span specimens. Suleiman's results were based on a shear-bond mode of failure for both static and repeated loading in comparison to the embossment tearing observed in these tests. It appears that specimens which fail in shear-bond when subjected to static and repeated loading should not require any further reduction factors when designing for warehouse applications, since standard factors of safety usually reduce the load to approximately 50 to 60% of the ultimate failure load [12,15]. The results obtained by other researchers [9,12] verify the behaviour of composite slabs to be adequate when subjected to repeated loading which causes shear-bond failure. Deck products with embossments in the bottom flange are subject to a different mode of failure which is more dependent on factors such as embossment details, environmental conditions (i.e. corrosion), etc. in determining fatigue strength.

It is interesting to note that two different failure modes are possible when composite slabs are subjected to repeated loading. Based on the results of all studies to date [9,12,15,16] it is advised that any composite slab could fail in either mode when subjected to the appropriate support and loading conditions. By simply changing the span length, it should be possible to invoke a different mode of failure in a composite slab, the critical length being dependent upon a number of variables such as embossment geometry and location, steel deck depth, etc. In the specific case used in this study, it is estimated that by shortening the span, shear-bond failure would be possible when subjected to repeated loading.

The stress-life procedure was chosen for analysis of the fatigue test results where results for first run specimens were plotted on a S–N curve incorporating $\log S_{max}$ versus $\log N_f$ where S_{max} is the maximum measured stress in the central bottom flange of the steel deck at the initial loading and N_f is the number of cycles endured at failure. The resulting S–N curve is shown in Figure 13. Due to the small number of tests, a log–log plot was chosen for displaying the test results and a fitted straight line was used to define the S–N curve. From the S–N curve, a nominal stress of 180 MPa can be estimated for a fatigue life of 1.25 million cycles. The fatigue strength is based on the nominal maximum stresses measured on the flat portion of the bottom centre flange of the deck.

Only first run specimens were considered in the stress-life analysis. The lack of fatigue data on which to make a comparison based on accumulated damage [19] made it difficult to include the results of tests which had been subjected to a previous stress history at a lower load. This would also be the case for the left and right bottom flanges which failed following the initial failure of the centre flange. From the results shown here, it is recommended that design standards for composite slabs incorporate checks on the maximum allowable stresses in composite slabs which are based on the particular deck type and geometry.

REFERENCES

[1] Ekberg, C. E., Jr. and Schuster, R. M., "Floor Systems with Composite Form-Reinforced Concrete Slabs", Final Report, International Association for Bridge and Structural Engineering, 8th Congress, New York, N.Y., Sept. 1968, pp. 385-394.

[2] Porter, M. L. and Ekberg, C. E., Jr., "Design Recommendations for Steel Deck Floor Slabs", *Journal of the Structural Division ASCE,* Vol. 102, No. ST 11, Proc. Paper 12528, November 1976, pp. 2121-2136.

[3] Porter, M. L., Greinmann, L. F., Elleby, Ekberg, C. E., Jr., "Regression Analysis for Prediction of Shear-Bond Failure of One-Way Slab Elements Reinforced with Cold Formed Steel Decking", Progress Report 23, Engineering Research Institute, Iowa State University, Ames, Iowa, July 1974.

[4] Schuster, R. M. and Ekberg, C. E., Jr., "Commentary on the Tentative Recommendations for the Design of Cold-Formed Steel Decking as Reinforcement for Concrete Floor Slabs", Engineering Research Institute, Iowa State University, Progress Report No. 8, ERI 79600, mes, Iowa, August 1970.

[5] Schuster, R. M., "Composite Steel-Deck Concrete Floor Systems", *Journal of the Structural Division, ASCE*, Vol. 102, No. ST5, Proc. Paper 12116, May 1976, pp. 899-917.

[6] ACI-ASCE Committee 326, "Shear and Diagonal Tension", Proceedings, American Concrete Insitute, Vol. 59, Jan., Feb. and March 1962, pp. 1-30, 277-334, and 353-396.

[7] Seleim, S. S. and Schuster, R. M., "Shear-Bond Capacity of Composite Slabs", Sixth International Specialty Conference on Cold-Formed Steel Structures, St. Louis, Missouri, No. 1982, pp. 511-531.

[8] Schuster, R. M., "Strength and Behaviour of Cold-Rolled Steel-Deck Reinforced Concrete Floor Slabs", thesis presented to the Iowa State University at Ames, Iowa, in 1970, in partial fulfillment of the requirements for the degree of Doctor of Philosophy.

[9] Abdel-Sayed, G., Temple, M. C. and Madugula, M. K. S., "Response of Composite Slabs to Dynamic Loads", Canadian Journal of Civil Engineering, Vol. 1, No. 1, 1974, pp. 62-70.

[10] Borowski, R., Bryman, M. and Hendrata, C., "Strength and Behaviour of Composite Steel-Deck Reinforced Concrete Floor Slabs Subjected to Repeated Loads", Report prepared at University of Waterloo, March 1977.

[11] Climenhaga, J. J. and Johnson, R. P., "Fatigue Strength of Forms Reinforced Composite Slabs for Bridge Decks", Publications, I.A.B.S.E., 35-1, 89-101, 1975.

[12] Mouw, Kenneth W., "Fatigue Testing of Light Metal Forms", Engineering Research Institute, Iowa State University, Ames, Iowa, January 1969, ERI-348, Project 741.

[13] Porter, M. L., "The Behaviour and Analysis of Two-Way Simply Supported Concrete Composite Floor Slabs Constructed with Cold-Formed Steel Decking", Ph.D. Thesis, Iowa State University, Ames, Iowa, 1974.

[14] Schuster, R. M. and Suleiman, R. E., "Composite Slabs Subjected to Repeated Point Loading", Eighth International Specialty Conference on Cold Formed Steel Structures, St.Louis, Missouri, U.S.A., Nov. 1986, pp. 453-485.

[15] Suleiman, R. E., "Behaviour of Composite Slabs Subjected to Repeated Point Loading", M.A.Sc. Thesis, University of Waterloo, Waterloo, Ontario, Canada, 1983.

[16] Temple, M. C. and Abdel-Sayed, G., "Fatigue Experiments on Composite Slab Floors", Proceedings of the Fourth International Specialty Conference on Cold-Formed Steel Structures, University of Missouri-Rolla, Mo., June 1978, pp. 871-891.

[17] McCuaig, L. A., "Strength And Behaviour of Composite Floor Slabs Subjected to Repeated Point Loading", M.A.Sc. Thesis, University of Waterloo, Waterloo, Ontario, Canada, 1986.

[18] Murdock, J. W., "A Critical Review of Research on Fatigue of Plain Concrete", Bulletin No. 475, Engineering Experiment Station, University of Illinois, Urbana, 1965.

[19] Miner, M. A., "Cumulative Damage in Fatigue", *Journal of Applied Mechanics,* Volume 12, September 1945.

[20] CSA Standard A23.3-M77, "Design of Concrete Structures for Buildings", Construction Standards Association, Rexdale, Ontario, Canada, 1977.

NOTATIONS

B Total width of composite slab, *mm*

D Overall depth of composite section, *mm*

d Depth from extreme compression fibre to centroidal axis of steel deck, *mm*

f_c' Compressive test concrete cylinder strength, MPa

K_t Stress concentration factor

L Length of span between supports, *mm*

L' Length of shear span, *mm*

N_f Cycles endured at time of fatigue failure

N_T Total cycles endured at time of test stoppage

P_D Computed dead load, *kN*

P_e Experimental load at any time during test, *kN*

P_{mr} Maximum repeated load, *kN*

P_{uc} Experimental cracking load in static test to failure, *kN*

P_{ue} Ultimate experimental static load from first static cycle, *kN*

P_{ur} Ultimate experimental static load after application of N cycles of repeated load, *kN*

S_{max} Maximum stress in deck flange at P_m, MPa

WL Weighted load factor for determination of maximum cyclic loads

Δ_e Experimental strain on flat portion of bottom flange, $10^{-6} m/m$

Δ_{es} Measured end-slip deflection, *mm*

Δ_f Final deflection at P_{mr} after N_t cycles of load, *mm*

Δ_i Initial deflection at P_{mr} after one static cycle, *mm*

Δ_p Permanent deflection due to cyclic creep, mm

ΔS_n Experimentally determined nominal stress, MPa

Δ_{ue} Midspan deflection at utlimate static failure, mm

Δ_ε Experimental strain at embossment location, $10^{-6}\, m/m$

Δ_σ Fluctuation in stress during cycling, MPa

Table 1: Results of Single and Double Span Static Load Tests

Specimen Identification	Concrete Strength f_c' *MPa*	Cracking Load P_{uc} *kN*	Ultimate Load P_{ue} *kN*	Load per Unit Width *kN/m*	End-Slip Δ_{es} *mm*	Midspan Deflection Δ_{ue} *mm*	Failure Mode
Single Span							
R-1-SS-SW (1)	22.8	62.3	65.7	71.8		11.2	Shear-Bond
R-1-SS (1)	29.4	103	112	62.3	3.20	12.8	Shear-Bond
R-2-SS (2)	21.3	92.5	98.8	54.0	5.40	11.2	Shear-Bond
Double Span							
R-1-DS (1)	27.0	106	117	63.9	4.70	11.4	Shear-Bond
R-1-DS-A (1)	27.0	103	117	63.7	4.80	15.7	Shear-Bond

Note (1) Embossment depths (flange - 1.83 mm; web - 1.59 mm)
(2) Embossment depths (flange - 1.58 mm; web - 1.50 mm)

Table 2: Results of Single Span Repeated Load Tests

Specimen Identification	Concrete Strength f_c' MPa	Load Characteristics: Maximum Load P_{mr} kN	Load per Unit Width P_{mr}/B kN/m	Load Ratio P_{mr}/P_{ue}	Cycles to Failure N_f Kc	Total Cycles N_T Kc	Deflection Characteristics: Permanent Δ_p mm	Maximum Δ_i mm	Maximum Δ_f mm	Failure Mode
R-3-SR (2)	24.6	67.0	36.6	0.60	500	782	2.40	4.41	7.20	Metal Fatigue
R-4-SR (2)	25.0	60.0	32.8	0.55		1250	2.01	3.60	5.75	
		63.8	34.9	0.58	2500	3896	2.45	5.99	6.58	Metal Fatigue
R-5-SR (1)	28.5	63.8	34.9	0.58	725	891	2.19	3.90	7.16	Metal Fatigue
R-6-SR (2)	25.1	63.8	34.9	0.58	200	516	2.51	4.18	7.18	Metal Fatigue
R-7-SR (1)	28.9	60.0	32.8	0.55	1250	2150	1.84	3.35	5.22	Metal Fatigue
R-8-SR (2)	30.6	63.8	34.9	0.58		1250	2.44	3.76	6.07	
		77.0	42.1	0.69	1354		3.02	6.79	7.81	Metal Fatigue
R-9-SR (2)	31.0	67.0	36.6	0.60	450		2.24	3.94	6.67	Metal Fatigue

Note (1) Embossment depths (flange - 1.83 mm; web - 1.59 mm)
(2) Embossment depths (flange - 1.58 mm; web - 1.50 mm)

Table 3 : Results of Double Span Repeated Load Tests

Specimen Identification	Concrete Strength f_c' MPa	Load Characteristics			Cycles to Failure N_f Kc	Total Cycles N_T Kc	Deflection Characteristics			Failure Mode
		Maximum Load P_{mr} kN	Load per Unit Width P_{mr}/B kN/m	Load Ratio P_{mr}/P_{ue}			Permanent Δ_p mm	Maximum Δ_i mm	Maximum Δ_f mm	
R-2-DR (2)	28.9	63.8	34.9	0.55		1250	1.87	3.16	5.22	
		67.0	36.6	0.57		2500	2.24	5.38	5.76	
		73.2	40.0	0.63		3500	2.60	6.05	6.65	
		80.0	43.7	0.68	4140		3.44	7.01	9.16	Metal Fatigue
R-2-DR-A (2)	28.9	80.0	43.7	0.68	433		2.92	4.92	9.72	Metal Fatigue
R-3-DR (2)	30.1	70.0	38.3	0.60		1250	1.86	3.30	5.56	
		75.0	41.0	0.64	1647	1660	2.36	5.51	6.25	Metal Fatigue
R-3-DR-A (2)	30.1	75.0	41.0	0.64	704	780	2.81	3.98	7.48	Metal Fatigue

Note (1) Embossment depths (flange - 1.83 mm; web - 1.59 mm)
(2) Embossment depths (flange - 1.58 mm; web - 1.50 mm)

Table 4: Strength and Deflection Data Following Fatigue Failure

Specimen Identification	Number of Cracked Flanges	Deflection		Ultimate Load P_{ur}	Load Ratio $\frac{P_{ur}}{P_{ue}}$
		Test Start *mm*	Failure *mm*	*kN*	
R-4-SR (2)	3	5.45	13.7	63.0	0.56
R-5-SR (1)	4	3.97	16.3	77.0	0.69
R-6-SR (2)	2	4.07	17.7	78.7	0.71
R-7-SR (1)	2	2.90	15.1	97.1	0.87
R-9-SR (2)	1	2.21	15.0	109	0.97
R-2-DR (2)	1	3.27	19.1	118	1.01
R-2-DR-A (2)	2	2.92	17.5	107	0.91
R-3-DR (2)	1	2.30	13.0	122	1.04
R-3-DR-A (2)	1	3.10	14.0	116	0.99

Note (1) Embossment depths (flange - 1.83 mm; web - 1.59 mm)
(2) Embossment depths (flange - 1.58 mm; web - 1.50 mm)

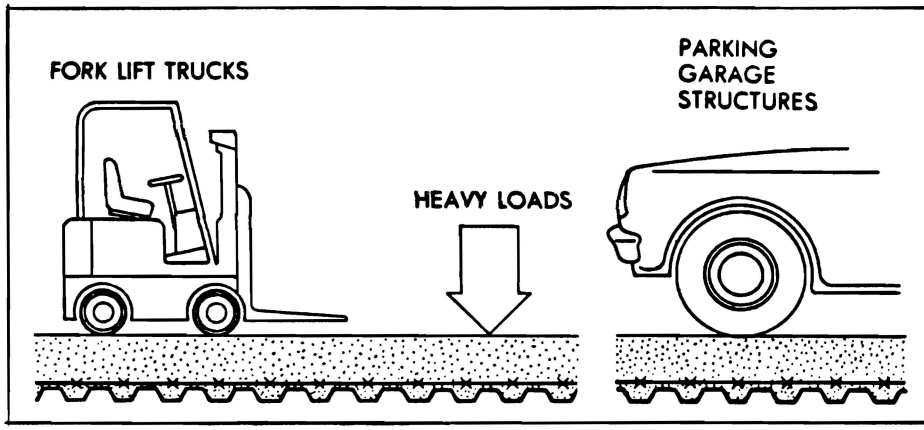

Figure 1. Schematic of Typical Composite Slab Floor System

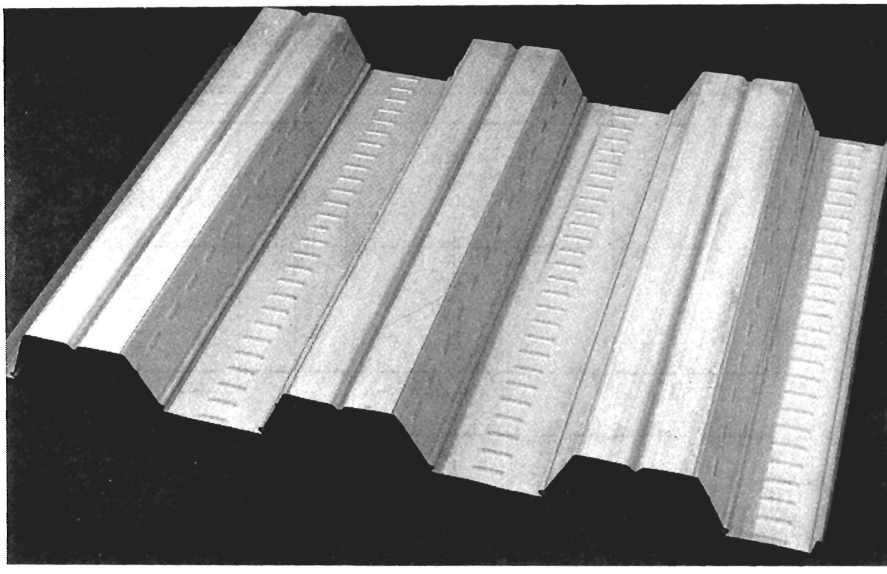

Figure 2. Photograph of Composite Steel Deck Tested

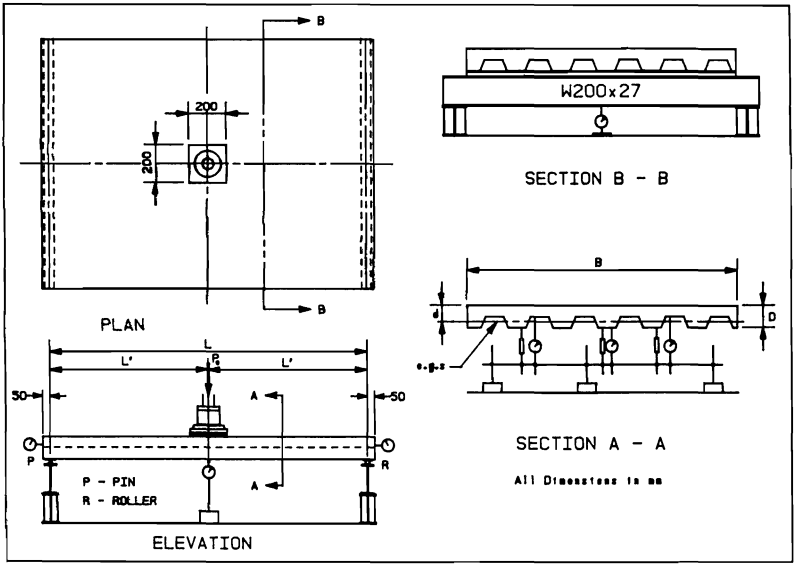

Figure 3. Schematic of Test Set-Up For Single Span Specimens

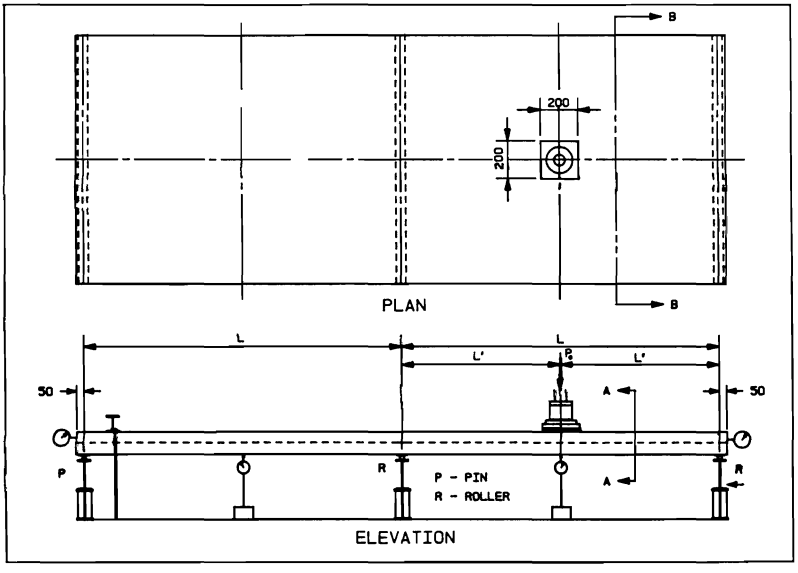

Figure 4. Schematic of Test Set-Up for Double Span Specimens

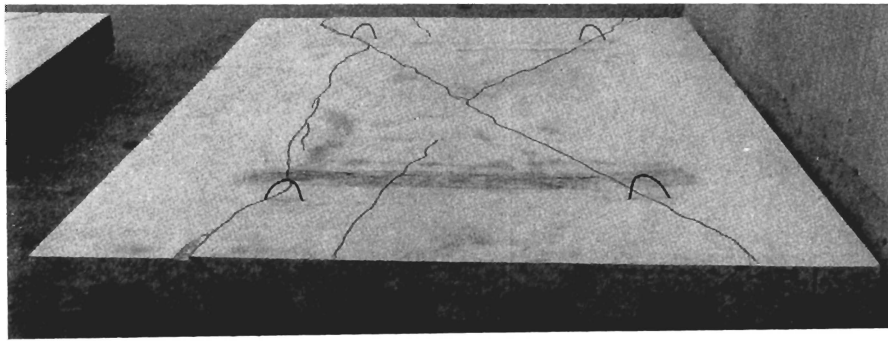

Figure 5. Crack Pattern of Single Span Specimen R-1-SS

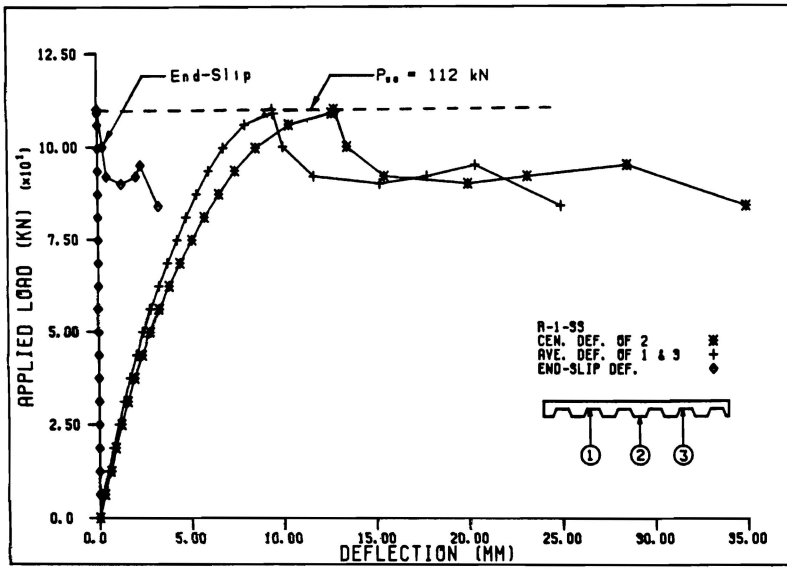

Figure 6. Load Deflection Behaviour of Specimen R-1-SS

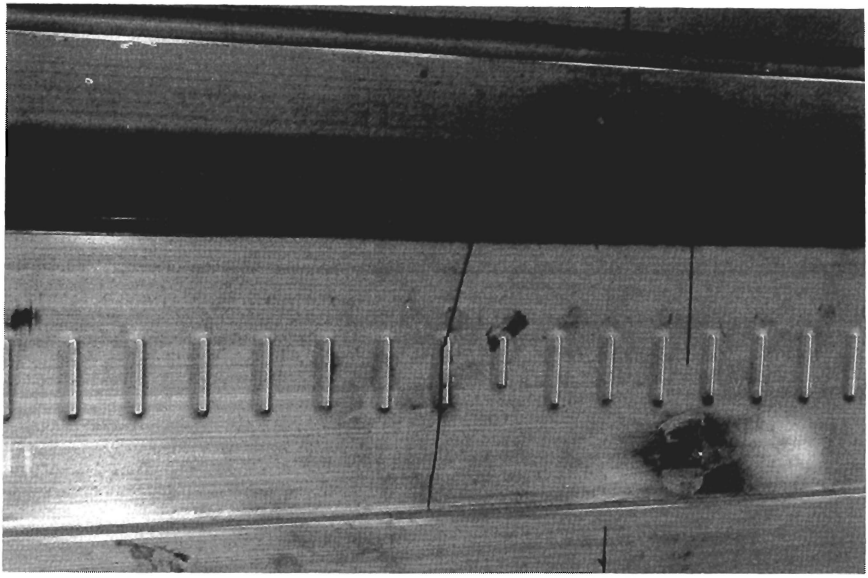

Figure 7. Close-up of Typical Embossment Fatigue Crack of Specimen R-3-SR

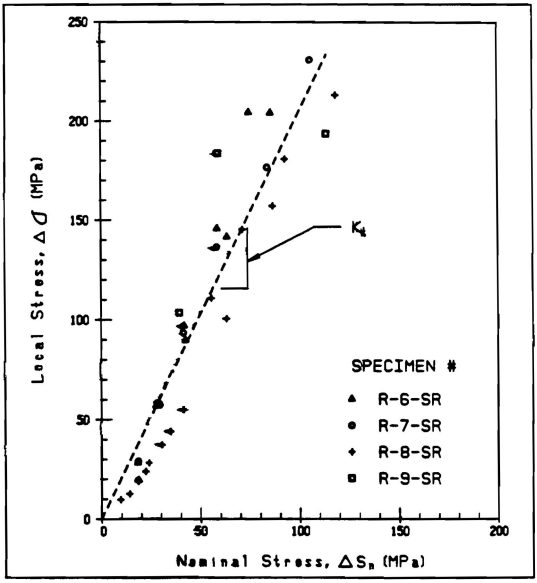

Figure 8. Comparison of Stress Concentrations of Typical Specimens Tested

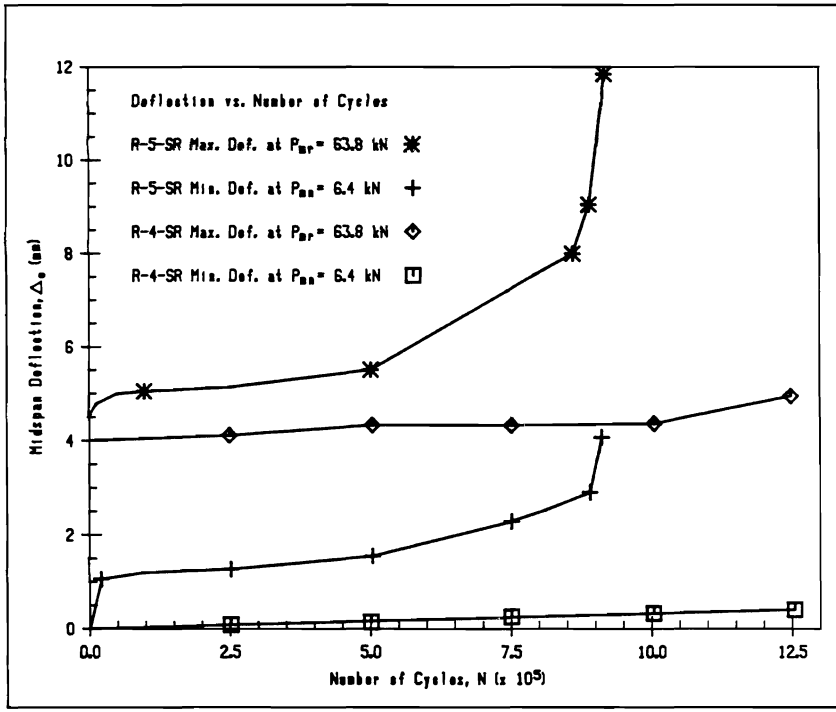

Figure 9. Illustration of "Coaxing" of Specimens R-4-SR and R-5-SR

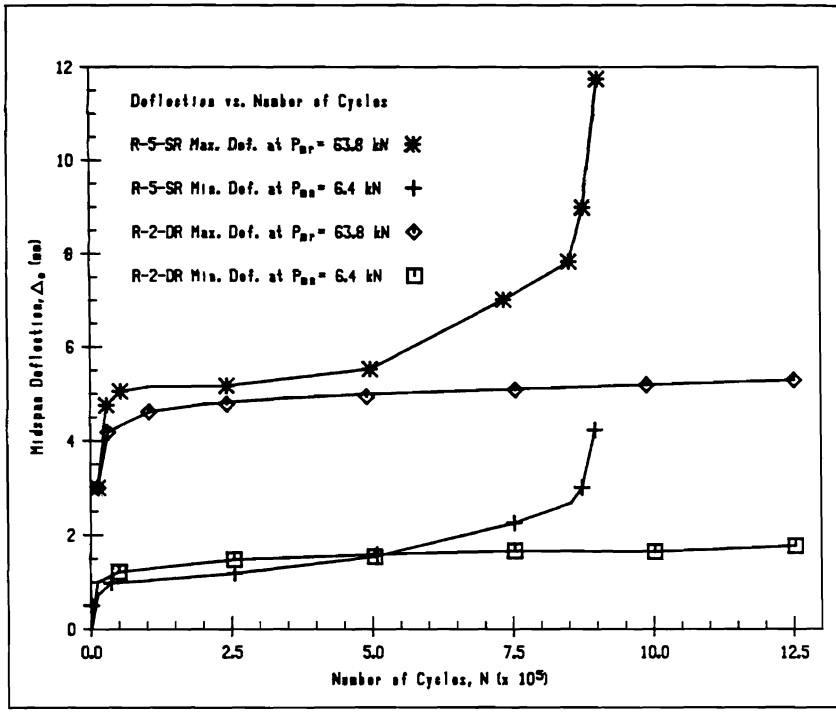

Figure 10. Comparison of Single and Double Span Specimens R-5-SR and R-2-DR

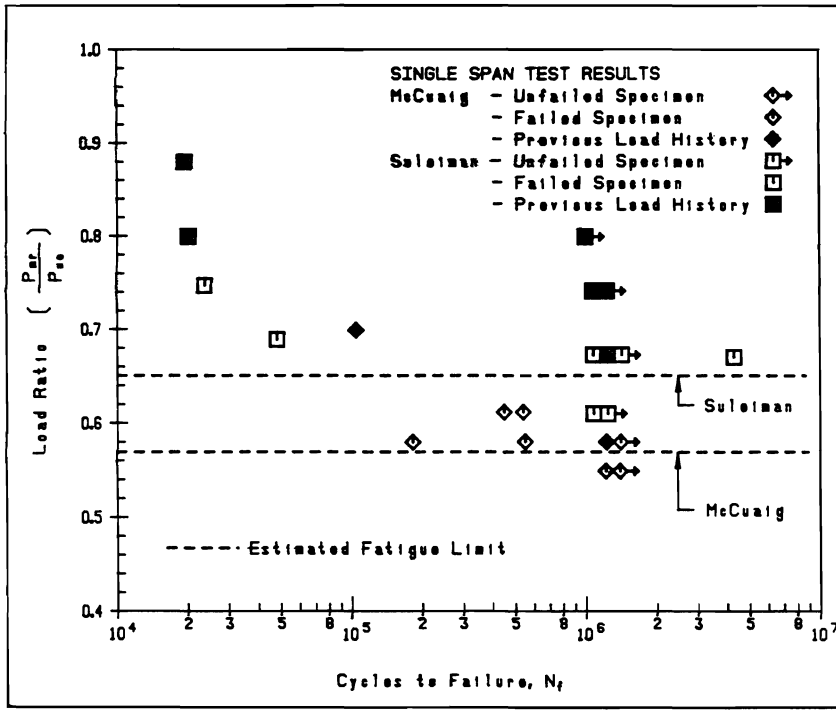

Figure 11. Load Ratio-Cycle Relationship of Single Span Specimens

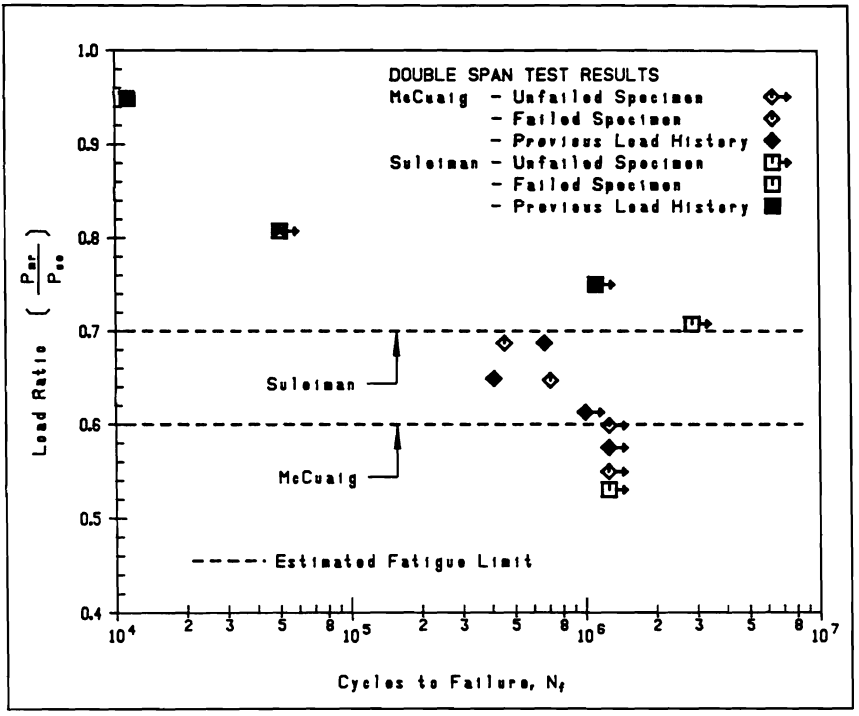

Figure 12. Load Ratio-Cycle Relationship of Double Span Specimens

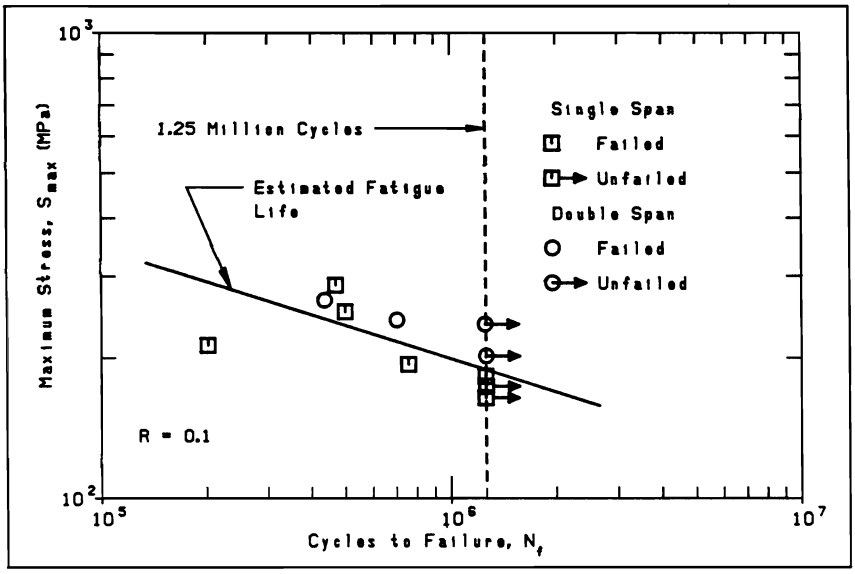

Figure 13. S-N Curve of Composite Slabs Subjected to Repeated Point Loading